



Application of combined physicochemical techniques for the efficient treatment of olive mill wastewaters

S.S. Kontos^{a,*}, P.G. Koutsoukos^a, C.A. Paraskeva^{a,b}

^aDepartment of Chemical Engineering, University of Patras, Rion, Patras GR 26504, Greece, Tel. + 30 2610 996219; Fax: + 30 2610 997574; emails: spyretos@chemeng.upatras.gr (S.S. Kontos), pgk@chemeng.upatras.gr (P.G. Koutsoukos), takisp@chemeng.upatras.gr (C.A. Paraskeva)

^bInstitute of Chemical Engineering Sciences, Foundation for Research and Technology, Hellas (FORTH/ICE-HT), Stadiou Str., Platani, Patras GR 26504, Greece

Received 10 March 2015; Accepted 7 June 2015

ABSTRACT

Olive Mill Wastewaters (OMW), produced from olive processing for the extraction of olive oil by units scattered in the Mediterranean countries, is a hardly degradable byproduct due to very high concentration of organic load of complex composition. Several treatment methods have been proposed for the efficient treatment of OMW, but because of the high operational cost, the application of these methods seems to be prohibitive, as olive mills are small family units and operate only 3–4 months per year. In the present work, the implementation of a combination of physicochemical treatment methods is proposed for the effective treatment of OMW. Initially, a membrane filtration process was used (ultrafiltration, nanofiltration, and reverse osmosis membranes) for the fractionation of OMW in concentrate and permeate streams. OMW was thus sufficiently treated and as a result the final permeate of the reverse osmosis was a pure water stream appropriate for irrigation purposes or for reuse in the OMW premises. The concentrated fraction from NF and RO membranes was further treated, to separate and isolate carbohydrates and the phenolic compounds, through the implementation of adsorption on specific resins. Alternatively, the enriched in phenolic content concentrated fractions could be investigated for the possibility of their selective recovery from the respective solution by cooling crystallization, applied directly to the concentrated fractions. During this process, it is possible to recover a number of components from their solutions according to the respective freezing points. Two Poly-Phenols (PP) contained in the OMW, namely trans-cinnamic acid (TCA) and ferulic acid (FA) were examined for the possibility of their selective extraction from their aqueous solutions by cooling crystallization, in order an operational model of the process to be developed. Initially, short cooling crystallization experiment cycles were done to test the effect of molecular diffusion and convection phenomena to the total PP recovery. Furthermore, crystallization of FA and TCA was followed during one cooling cycle as a function of time past the immersion of a cold surface in hot homogeneous solutions of the test compounds. It was estimated that in the case of mixtures, a total recovery of 66% FA and 50% TCA was achieved. The

*Corresponding author.

Presented at the 7th International Conference on Water Resources in the Mediterranean Basin (WATMED7) 8–11 October 2014, Marrakesh, Morocco

combination of membrane filtration and cooling crystallization may be quite promising for the development of more effective and integrated exploitation of OMW abiding to the zero waste targets.

Keywords: Olive mill wastewaters; Phenolic compounds; Membrane filtration; Cooling crystallization

1. Introduction

Olive oil production is of paramount importance for the economic prosperity of many Mediterranean countries. Due to the antioxidant activity of phenolic compounds contained in OMW, a number of researchers have demonstrated that their isolation and subsequent use in the food industry and in pharmaceuticals may have beneficial effects toward a number of human disease, including gastric and intestinal digestion and atherosclerosis [1,2]. On the other hand, the uncontrolled disposal of the produced wastewaters into aquatic receptors has serious environmental consequences leading to water pollution, contamination, eutrophication, etc. [3]. The development of cost-effective methods for the efficient treatment of OMW is of paramount importance for all Mediterranean countries, engaged in the olive oil production [4]. The main treatment methods, applied so far apart from direct OMW disposal, are mainly the physicochemical and biological treatment methods. Physicochemical treatment methods include coagulation/flocculation, membrane filtration, and adsorption-desorption on selective resins and cooling crystallization. Coagulation/flocculation is a rapid and relatively low-cost process for the reduction of mainly total suspended solids and part of the organic load [5]. Membrane filtration has been applied for the purification of various agro-industrial wastes including OMW. Paraskeva et al. [6,7] and Zagklis et al. [8] implemented membrane technology in order to investigate the possibility of complete fraction of OMW by carrying out a detailed parametric study. It was suggested that the ultrafiltration process resulted in the separation of high molecular weight constituents, whereas the phenolic content, present in OMW, was highly concentrated at the nanofiltration step. The high phenol content concentrates were tested in hydroponic systems and it was shown that they favored the development of native plants while they prevented undesired development of herbs [7]. Cassano et al. evaluated the performance of different ultrafiltration membranes for the efficient treatment of OMW [9]. At the laboratory scale, they suggested an integrated membrane system consisting of two ultrafiltration steps followed by a nanofiltration step. High levels of purification were

achieved rendering the final permeate appropriate for irrigation or for feedback in the olive oil extraction process [10]. Stoller and Chianese examined the purification of olive washing wastewaters by operating batch membrane processes taking into account associated fouling phenomena. It was reported that membrane processes should operate at pressures which cause permeate fluxes lower or equal to the critical one leading to successfully reduced fouling [11]. Zagklis and Paraskeva presented a method for the exploitation of agro-industrial wastes, OMW and defect wine, by applying a combined system of membrane filtration and rotary evaporation of concentrated fractions, resulting in the isolation of low molecular weight compounds (phenols and simple carbohydrates) from the initial waste [12]. For further isolation and purification of phenolics, Zagklis et al. employed reverse osmosis in addition to the nanofiltration step in order to concentrate simple phenolic compounds and mono or disaccharides in the concentrate stream of reverse osmosis process. Isolation of phenolics was done by adsorption/desorption in resins (non ionic XAD4, XAD16, and XAD7HP resins). The final results were very promising leading to a high recovery of phenolic compounds, through vacuum evaporation, reaching values equal to 84.8 g/L of hydroxytyrosol [8], whereas the initial total phenolic concentration in raw OMW was 2.64 g/L.

The need for selective recovery of high-added value products (e.g. phenolic compounds), present in OMW, led to the implementation of a cooling crystallization process, in which the various components may be separated from the respective solution according to their freezing/melting point. This particular treatment method has been industrially applied by a number of researchers for the isolation of high-added value compounds. Specifically, Chianese and Santilli developed a mathematical simulation for the calculation of the solid-layer growth as a function of time for the systems of pure ϵ -caprolactam, pure naphthalene, and mixtures of ϵ -caprolactam and water [13]. Kim and Ulrich proposed an experimental procedure and a simulation model to calculate the crystalline layer growth in a layer melt crystallization for the binary system of caprolactam and water. The final output

seemed to be very encouraging, showing very good matching of the experimental data with molecular simulations [14]. Recently, Kontos et al. investigated the possibility of extracting purified high-added value products (e.g. polyphenols) from OMW. To further research this issue, two representative polyphenols, namely trans-cinnamic acid and ferulic acid (FA), present in OMW, were selected as a model system for the investigation of their recovery from aqueous solutions by cooling crystallization. The driving force for crystallization was mass diffusion in unstirred solutions/melts. The cold temperature, T_{cold} , of the cooled surface increased supercooling, $\Delta T = T_{\text{melt}} - T_{\text{cold}}$, leading to a higher concentration difference corresponding to solubility variation with temperature of the test compounds. Apparently higher concentration difference of the test substances existed near the cold surface. Each cooling cycle lasted for 5 min and within this period the experimentally deposited crystal mass was measured compared with the theoretically calculated in terms of layer thickness. For each of the tested phenols, the agreement was excellent [15].

In the present work, cooling crystallization cycles were carried out in stirred solutions in order to examine the effect of convection phenomena in the total PP recovery. The experimental results were compared with the results obtained for crystallization controlled by diffusion conditions [15]. The efficiency of the method was evaluated from preliminary experiments using mixtures of FA and trans-cinnamic acid (TCA). The quantitative results, targeted in the present work, aimed at the development of an integrated management procedure for OMW. The target may be achieved through the combination of several physico-chemical treatment methods with the recovery of the phenolic compounds from the concentrates on a cooled surface.

2. Materials and methods

2.1. Determination of TCA and FA in the solid–crystal layer

Synthetic crystalline PPs, TCA, and FA were obtained from Sigma–Aldrich (99% purity). The quantitative analysis of FA in solutions was done by the spectrophotometric Folin-Ciocalteu method [16] at wavelength of 760 nm. TCA concentrations were measured by titrations with 0.1 N NaOH, using ethanol as solvent [17].

2.2. Crystallization process

The apparatus used for the crystallization experiments is shown in Fig. 1, and has been recently described in details elsewhere [15]. A water jacketed

double walled Pyrex[®] glass vessel of inner diameter 6.5 cm and active volume 250 mL, was used as the reactor for the crystallization experiments. The temperature at the walls of the reactor was kept constant and equal to T_{hot} by circulating water from a thermostat. The temperature, T_{hot} , at the walls of the reactor was sufficiently higher from the melting temperature, T_{melt} , in order to ensure full dissolution of the test PPs in the water. In the same way, the temperature, T_{cold} , of the cooled cylindrical surface was kept constant by the circulation of cold water in the inner side of the cylinder ($\varnothing = 25$ mm, $L = 120$ mm), supplied from a heat exchanger.

The experimental process followed the next steps: Initially, the reactor temperature was raised up to temperature, T_{hot} , for the complete dissolution of the test PPs in triply distilled water. Next, the cooled surface (at temperature T_{cold}) was immersed in the PPs' solution. Past up to 600 min from the onset of crystallization, the cylinder was removed and the crystals formed were left overnight to dry on the cold surface at room temperature. The mass crystallized was measured by dissolving the crystals in water and analysis for PP content as already described.

3. Results and discussion

3.1. Optimal conditions for the cooling crystallization experiments of the test PPs

The prerequisite for nucleation and crystal growth is the establishment of supersaturation in the solution. In the present work, the differences of the solubility of the test PPs as a function of temperature was used for the formation of supercooled solutions from which nucleation and crystal growth could take place. Solubility gradients were imposed through the maintenance of large temperature differences between the walls, T_{cold} , and the walls of the reactor, T_{hot} . An important task of the present work was the application of an optimum temperature gradient, $T_{\text{hot}} - T_{\text{cold}}$, ensuring sufficient concentration difference of the PPs between the walls and the cooled surface. The freezing points of aqueous solutions of FA and TCA were measured experimentally [15]. The initial concentrations of FA and TCA were 3 and 1 gL⁻¹, respectively, corresponding to melting points of 58 and 54°C. Setting $T_{\text{hot}} = 70^\circ\text{C}$, the PPs were completely dissolved. Regarding the temperature of the cooled surface, T_{cold} , it was set to 5°C corresponding to equilibrium solubility of 0.15 gL⁻¹ for both PPs. The applied temperature values of T_{hot} and T_{cold} , imposed a sufficiently large temperature gradient to the system, leading to a higher supercooling value, $\Delta T = T_{\text{melt}} - T_{\text{cold}}$, resulting

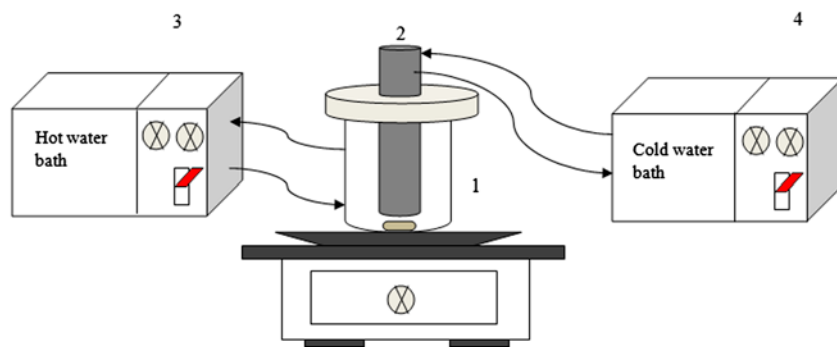


Fig. 1. Experimental setup for the cooling crystallization process: (1) batch reactor, (2) cooled cylindrical surface, (3) hot thermostat, and (4) cryostat.

to the formation of more crystallites (close to the cooled surface), where a sufficiently large concentration difference was established. The cooling crystallization experiments of the present work, involved 40 immersions (cooling cycles) of the cooled surface in the stirred PP solutions. Each cooling cycle lasted for 5 min, time sufficient for the formation of crystals. The results were compared with results obtained at diffusion conditions in unstirred solutions [15].

A series of experiments in the present work involved a cooling cycle which lasted for 5 h. Similar processes for the purification of a number of compounds have been adopted by several researchers [13,18]. The procedure adopted at the present work aimed at the development of a model for the efficient recovery of PPs by cooling crystallization on the industrial scale.

3.2. Comparative presentation of cooling crystallization experiments of FA 3 gL^{-1} from a superheated solution in the presence and absence of stirring

In the current set of experiments, in order to investigate the effect convective phenomena in the total recovery of FA from a supersaturated solution of initial concentration 3 gL^{-1} , 40 sequential immersions of the cooled surface were carried out at different rotation speeds of the magnetic stirrer ($\omega = 0, 80, 150 \text{ rad min}^{-1}$) for $T_{\text{cold}} = 5^\circ\text{C}$ as may be seen in Fig. 2.

The experimental results for the recovery of FA for different applied rotational velocities of the solution ($\omega = 0, 80, 150 \text{ rad min}^{-1}$) are summarized in Table 1.

As may be seen in Table 1, it was found that upon increasing fluid rotational value, FA recovery decreased, contrary to expectations that higher velocity would result to more homogeneous solutions and higher amounts of the crystallized substance on the cold surface. In order to understand this behavior, a theoretical study of the momentum of r , θ , and z axis

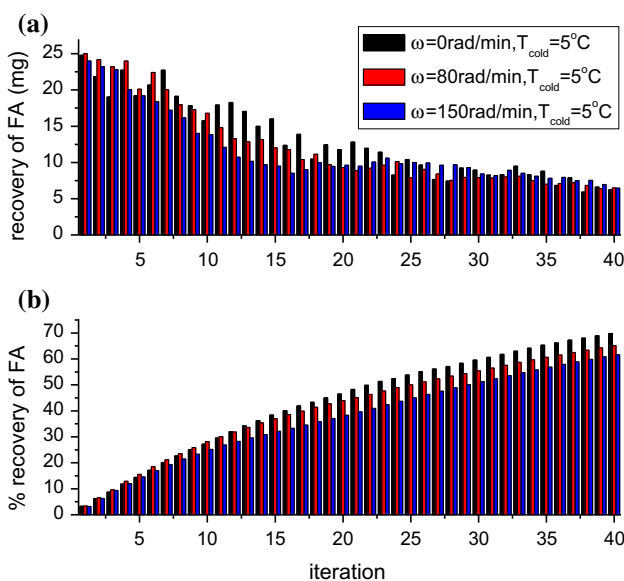


Fig. 2. (a) Recovery per cooling cycle and (b) total recovery of FA, at $T_{\text{cold}} = 5^\circ\text{C}$ for different rotational speed settings of the magnetic stirrer; $\omega = 0, 80, 150 \text{ rad} \times \text{min}^{-1}$.

was conducted, for the investigation of the height distribution, h , of the rotating fluid as a function of the distance, r , from the cooled surface. The layout of the system for which calculations have been done is shown in Fig. 3. Similar calculations have been done for a fluid in a reactor at rotational motion in the absence of the cooled surface [19].

The momentum analysis was examined in cylindrical coordinates. Initially, the simplification of r and θ momentums yielded to the computation of the rotational velocity, v_θ , as a function of the radius, r . Next, the substitution of the v_θ , to the simplified z -momentum resulted in an equation showing the dependence of the height distribution, h , with the radius, r , for different rotational velocity settings of the magnetic stirrer. Specifically:

Table 1

Total recovery of FA for different values of rotational speed of magnetic stirrer (initial amount in solution 750 mg FA)

	$\omega = 0 \text{ rad min}^{-1}$	$\omega = 80 \text{ rad min}^{-1}$	$\omega = 150 \text{ rad min}^{-1}$
Recovered FA (mg)	523.4	488.25	462.2
% recovery	69.8	65.1	61.62

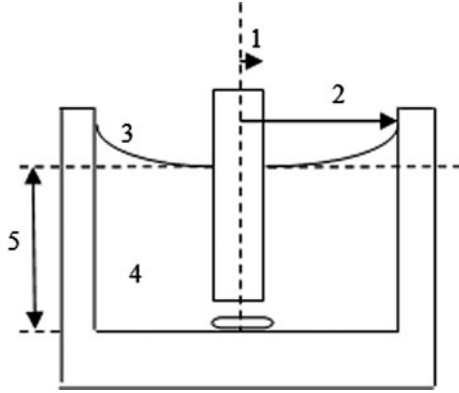


Fig. 3. Layout of the free interface (bulk solution-air) h as a function of the radius r : (1) internal radius of the cooled surface R_1 , (2) distance from the walls of the reactor R_2 , (3) on the free interface $P = P_{\text{atm}}$, (4) within the fluid, it holds $P = P(r, z)$, and (5) initial height of the free interface h_0 .

r -momentum:

$$\begin{aligned} & \rho \left(\frac{\partial v_r}{\partial t} + v_r \frac{\partial v_r}{\partial r} + \frac{v_\theta}{r} \frac{\partial v_r}{\partial \theta} - \frac{v_\theta^2}{r} + v_z \frac{\partial v_r}{\partial z} \right) \\ &= \mu \left\{ \frac{\partial}{\partial r} \left[\frac{1}{r} \frac{\partial}{\partial r} (rv_r) \right] + \frac{1}{r^2} \frac{\partial^2 v_r}{\partial \theta^2} + \frac{\partial^2 v_r}{\partial z^2} - \frac{2}{r^2} \frac{\partial v_\theta}{\partial \theta} \right\} - \frac{\partial P}{\partial r} + \rho g_r \\ &\Rightarrow -\rho \frac{v_\theta^2}{r} = -\frac{\partial P}{\partial r} \end{aligned} \quad (1)$$

θ -momentum:

$$\begin{aligned} & \rho \left(\frac{\partial v_\theta}{\partial t} + v_r \frac{\partial v_\theta}{\partial r} + \frac{v_\theta}{r} \frac{\partial v_\theta}{\partial \theta} - \frac{v_r v_\theta}{r} + v_z \frac{\partial v_\theta}{\partial z} \right) \\ &= \mu \left\{ \frac{\partial}{\partial r} \left[\frac{1}{r} \frac{\partial}{\partial r} (rv_\theta) \right] + \frac{1}{r^2} \frac{\partial^2 v_\theta}{\partial \theta^2} + \frac{\partial^2 v_\theta}{\partial z^2} + \frac{2}{r^2} \frac{\partial v_\theta}{\partial \theta} \right\} \\ &\quad - \frac{1}{r} \frac{\partial P}{\partial r} + \rho g_\theta \Rightarrow \mu \frac{\partial}{\partial r} \left[\frac{1}{r} \frac{\partial}{\partial r} (rv_\theta) \right] = 0 \\ &\Rightarrow \frac{1}{r} \frac{\partial}{\partial r} (rv_\theta) = c_1 \Rightarrow \frac{\partial}{\partial r} (rv_\theta) = c_1 r \\ &\Rightarrow rv_\theta = c_1 \frac{r^2}{2} + c_2 \Rightarrow v_\theta = \frac{c_1}{2} r + \frac{c_2}{r} \end{aligned}$$

Boundary condition at the cooled surface was B.C.1: $v_\theta(r = R_1) = 0$ and the corresponding condition at the

wall of the reactor was set to B.C.2: $v_\theta(r = R_2) = \omega R_2$. The application of the BCs leads to the computation of the velocity profile in the θ -axis:

$$v_\theta = \frac{\Omega R_2^2}{R_1^2 - R_2^2} \left[\frac{R_1^2}{r} - r \right] \quad (2)$$

Substitution of Eq. (2) in Eq. (1) and integration of the resulting equation allowed the calculation of pressure dependence on r and z axis.

$$\begin{aligned} P(r, z) &= \frac{\rho \Omega^2 R_2^4 R_1^4}{(R_1^2 - R_2^2)^2} \left(-\frac{1}{2r^2} \right) - \frac{2\rho \Omega^2 R_1^2 R_2^4}{(R_1^2 - R_2^2)^2} \ln(r) \\ &\quad + \frac{\rho \Omega^2 R_2^4}{(R_1^2 - R_2^2)^2} \frac{r^2}{2} + g(z) \end{aligned} \quad (3)$$

Simplification of z -momentum, yielded:

$$-\frac{\partial P}{\partial z} - \rho g = 0 \quad (4)$$

Integration of z -momentum:

$$P(r, z) = -\rho g z + f(r) \quad (5)$$

The pressure on the interface is equal to $P_{\text{liquid}} = P_{\text{gas}} \Rightarrow P_l = P_{\text{atm}}$

Combining Eqs. (3) and (5):

$$\begin{aligned} P &= -\frac{\rho \Omega^2 R_1^4 R_2^4}{2(R_1^2 - R_2^2)^2} \frac{1}{r^2} - \frac{2\rho \Omega^2 R_1^2 R_2^4}{(R_1^2 - R_2^2)^2} \ln(r) \\ &\quad + \frac{\rho \Omega^2 R_2^4}{2(R_1^2 - R_2^2)^2} r^2 - \rho g z + c \xrightarrow{z=h(r)} \\ \Rightarrow \rho g h(r) &= -\frac{\rho \Omega^2 R_1^4 R_2^4}{2(R_1^2 - R_2^2)^2} \frac{1}{r^2} - \frac{2\rho \Omega^2 R_1^2 R_2^4}{(R_1^2 - R_2^2)^2} \ln(r) \\ &\quad + \frac{\rho \Omega^2 R_2^4}{2(R_1^2 - R_2^2)^2} r^2 + c - P \\ \Rightarrow h(r) &= -\frac{\Omega^2 R_1^4 R_2^4}{2g(R_1^2 - R_2^2)^2} \frac{1}{r^2} - \frac{2\Omega^2 R_1^2 R_2^4}{g(R_1^2 - R_2^2)^2} \ln(r) \\ &\quad + \frac{\Omega^2 R_2^4}{2g(R_1^2 - R_2^2)^2} r^2 + \frac{c - P}{\rho g} \end{aligned} \quad (6)$$

With

$$a = \frac{\Omega^2 R_1^4 R_2^4}{2g(R_1^2 - R_2^2)^2}, b = \frac{2\Omega^2 R_1^2 R_2^4}{g(R_1^2 - R_2^2)^2}, d = \frac{\Omega^2 R_2^4}{2g(R_1^2 - R_2^2)^2} \quad (7)$$

And considering that: $r = R_1$ and $h = h_o \rightarrow P = P_{atm}$, constant, c , could be computed.

Finally, the distribution of h at the interface was calculated from Eq. (8):

$$h(r) = h_o + a\left(\frac{1}{R_1^2} - \frac{1}{r^2}\right) + b \ln\left(\frac{R_1}{r}\right) + d(r^2 - R_1^2) \quad (8)$$

The profile of h on the interface as a function of the radius r is plotted in Fig. 4.

As may be seen from Table 1, it is clear that a sufficient increase in the fluid angular velocity may have negative effects on the final recovery of the deposited solid on the cold cylinder. Specifically, in the absence of stirring conditions, the overall recovery was up to 69.8%, whereas for fluid velocities $\omega = 80, 150 \text{ rad min}^{-1}$, crystallized solid was decreased to 65.1 and 61.6% with respect to the initially dissolved solid, respectively.

This conclusion was confirmed by the curves shown in Fig. 4. Increase in the applied fluid rotational speed, the respective curves were sharper, due to the fact that the molecules of dissolved PP did not have sufficient time to diffuse in the domain of concentration differences adequate for nucleation and crystal growth. The driving force for mass transfer mechanism is the convection, imposed to system

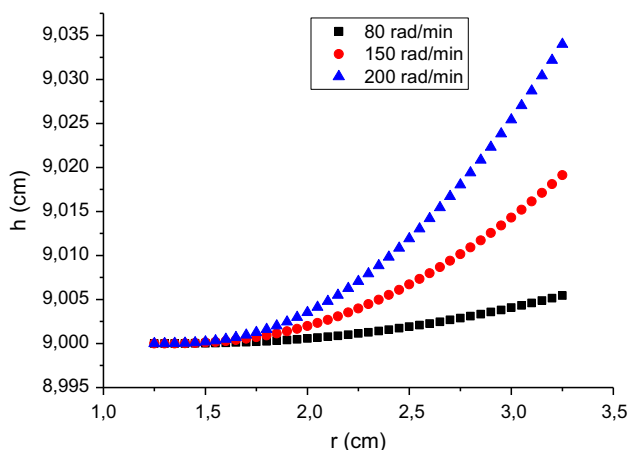


Fig. 4. Distribution of the interface of the bulk solution, h , as a function of the radius, r , for different angular rates of fluid flow.

through stirring rather than mass diffusion, resulting to a slight decrease in the PP recovery at the cooled surface which may be attributed to the fact that crystallization takes place in the bulk solution as well.

3.3. Crystallization of TCA and FA

Two-hundred and fifty milligrams of TCA were dissolved in a batch reactor of active volume of 250 mL (initial concentration 1 gL^{-1}) kept at $T_{hot} = 70^\circ\text{C}$. Upon immersion of the cold metallic surface cooled at temperature $T_{cold} = 5^\circ\text{C}$, crystallization was initiated and lasted for 5 h. The amount of solid crystallized was measured by titration with standard solution of 0.1 N NaOH. It was found that 126 mg TCA were recovered by crystallization, corresponding to 50.4% of the initial solid in the crystallizer.

For the case of FA, 750 mg FA (3 gL^{-1}) were weighted for the preparation of the stock solution. Hereupon, the same experimental process, as in the case of TCA, was followed. Past the removal of the cooled surface, the determination of the mass of the crystals formed was done by the Folin-Ciocalteu method [16], and also via titration with NaOH 0.1 N [17]. The recovered solid was 70% of the initial amount in solution. The recovery achieved by cooling crystallization, estimated with two different analytical procedures for TCA and FA is summarized in Table 2.

As may be seen from Table 2, there was a satisfactory agreement (within ca. 3%) between the two methods tested for the quantitative measurement of the amounts of the test PPs. Concerning TCA, as may be seen from Table 2, it was not possible to be measured by the Folin-Ciocalteu because the benzene ring of TCA cannot be associated with a hydroxyl radical as required by the latter analytical method [16].

3.4. Crystallization of mixture of FA and TCA in hot solutions by cooling crystallization

In the following set of experiments, crystallization of mixtures of FA and TCA were carried out for the investigation of their selective recovery from super-cooled solutions. The optimum crystallization conditions ($T_{hot} = 70^\circ\text{C}$, $T_{cold} = 5^\circ\text{C}$) were selected in order to impose a large temperature gradient in the test solution taking into account the variation of solubility of FA and TCA with temperature. In this series of experiments, solutions were cooled in the same way as the model FA and TCA solutions, in an attempt to examine the potential of the selective recovery of high-added value products (namely PPs, which have important applications as food additives, pharmaceuticals [1]).

Table 2

Summary of results obtained from two different methods for the determination of the amounts of TCA and FA recovered by cooling crystallization; $T_{\text{cold}} = 5^{\circ}\text{C}$, $t = 5\text{ h}$

$T_{\text{cold}} = 5^{\circ}\text{C}$, $t = 5\text{ h}$		
PolyPhenol	Titration with NaOH 0.1 N of the recovered solid (mg)	Folin-Ciocalteu method (mg)
TCA	126	n/a
FA	510.8	526

The cooling crystallization process involves the separation of a solute based on the reduction of its solubility with decreasing temperature. The solute in the form of crystalline material may be separated by deposition in the form of a layer on a cooled surface. The thickness of the deposited crystalline layer and the purity of the crystals separated from the mother liquor are important characteristics of the process.

3.4.1. Determination of the amounts of FA and TCA obtained by cooling crystallization

The solutions tested in the cooling crystallization experiments, contained FA and TCA at the same concentrations as the model solutions (3 gL^{-1} for FA and 1 gL^{-1} for TCA). The crystals formed on the cooled surface were calculated for three different time periods (50, 250, and 600 min) from the onset of crystallization and the respective amounts formed are summarized in Table 3.

As may be seen from Table 3, increase in the crystallization time yielded higher recovery rates for both FA and TCA. Similar results have been reported by Parisi and Chianese for other pair of compounds [18]. In order to investigate the possibility of higher recovery efficiencies, the total duration of crystallization was increased substantially, up to 10 h. The final results were very encouraging as they showed that recovery of 65.8 and 50.4% for FA and TCA, respectively, was achieved. In Fig. 5, the amounts of the solids recovered by cooling crystallization are shown.

As may be seen from Fig. 5, at the early stages of crystallization, the recovery was substantially high reaching a plateau after ca. 100 min for TCA and past

Table 3

Amount of FA and TCA recovered from solutions by cooling crystallization at different time periods past the onset of crystallization (Starting quantities 750 mg FA and 250 mg TCA)

	$t = 50\text{ min}$	$t = 250\text{ min}$	$t = 600\text{ min}$
FA (mg)	197.5	346	494
TCA (mg)	66.4	90	126

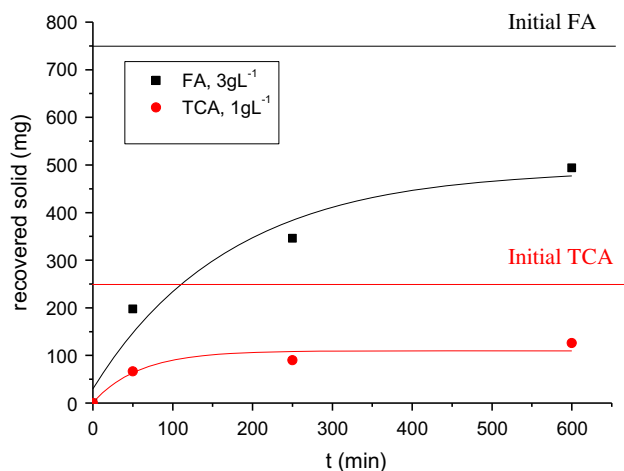


Fig. 5. Recovery of FA and TCA deposited on the cooled surface as a function of time of crystallization.

ca. 300 min for FA. The reduction of the deposited amounts with time (rate of crystallization reduction) is apparently associated with the concomitant decrease in the solution supersaturation with respect to the solutes studied. Crystallization proceeds until equilibrium is reached corresponding to the solubility of FA and TCA at temperature equal to T_{cold} .

3.4.2. Determination of water content entrapped in the crystal layer

The specification of the impurity content of the solid obtained by crystallization is a very important issue. The most likely impurity to be found in the crystal layers formed was water because of its excess (solvent). Water content in the crystalline samples obtained was measured with Karl-Fischer titrations [15,20] using anhydrous methanol as solvent. In all cases, the amount of water measured was insignificant and within experimental error.

The mass fractions of FA, TCA, and water measured past 50, 250, and 600 min upon the immersion of the cold surface, are shown in Table 4.

Table 4
Fraction of FA, TCA and water in the recovered solid

	$t = 50$ min	$t = 250$ min	$t = 600$ min
Mass fraction of FA	74.8	79.4	80
Mass fraction of TCA	25.2	20.5	20.4
Mass fraction of water	0.006	0.006	0.007

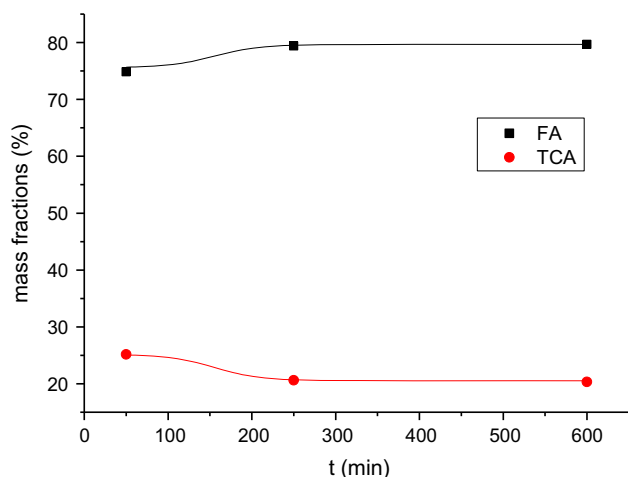


Fig. 6. Mass fractions of FA and TCA deposited on the cooled surface (5°C), as a function of the crystallization times.

As may be seen in Table 4, the mass fraction of FA increased slightly at longer crystallization times, whereas exactly the opposite trend was shown for TCA. Water quantities measured in the crystal layer were negligible, suggesting that the recovered crystals were very pure. The dependence of the mass of FA and TCA layers formed by cooling crystallization as a function of the crystallization time is shown in Fig. 6.

As already mentioned, TCA is of substantially lower amount when compared to FA in the original solution (initial amount in the solution 250 mg TCA and 750 mg FA). It is interesting to note that the mass fraction of TCA was larger in the first 50 min of crystallization suggesting higher incorporation rates of TCA in the early stages of crystallization. This observation may be attributed to the substantially high temperature gradient, applied to the system, favoring the incorporation of the lower amount compound, TCA, in the crystal layer in the beginning of the experiment. Similar results were, also, reported in the work of Parisi and Chianese [18] enhancing the entrapment of the impurity in solid layer at the first 50 min from the onset of crystallization.

3.5. Physicochemical treatment methods applied for the treatment of OMW

In order to investigate the possibility of extracting high-added value products from wastewaters, preliminary crystallization experiments with raw OMW were done. The experimental process, described in the crystallization of synthetic mixtures, was adopted. The experiments were conducted by applying the optimum temperature gradient to the bulk solution, which in this series of experiments was OMW. Specifically, at the walls of the reactor the temperature remained constant, $T_{\text{hot}} = 70^\circ\text{C}$ while the surface temperature of the cooled surface was equal to $T_{\text{cold}} = 5^\circ\text{C}$.

The two OMW samples of the current study were characterized and presented in a recent work of Iakovides et al. [5]. The characteristic high organic loading and phenolic content, in terms of COD and gallic acid, respectively, are shown in Table 5.

As may be seen from Table 5, measurements of the concentration of the organic load and the recovered phenolic content, of the solids deposited on the cooled surface, it was confirmed that the recovery of PP from raw OMW is not feasible without the required concentrated pretreatment of the waste as their particular solubility in the waste were far less than those needed for the development of favorable supersaturation [15]. The solubility of hydroxytyrosol in water is substantially high, whereas its concentration in OMW stream was found to be ca. 0.3 g L^{-1} [15]. As a matter of fact, it is clear that its recovery in crystalline form would not be viable, unless its concentration in the bulk solution is highly increased. A method suggested for the more efficient treatment of OMW should include sequential sieving through stainless steel filters for the removal of high molecular weight compounds, next, membrane technology should be implemented for the isolation of the high-added value byproducts contained in the concentrated streams of nanofiltration and reverse osmosis as demonstrated by a number of researchers [6,9]. In addition, the final permeate of the reverse osmosis may be used for irrigation purposes [7], while the enriched in phenolic fraction reverse osmosis concentrate may be further treated with the application of resins for the purification of phenolics

Table 5

Percentage of organic loading and phenolic content in the raw OMW and the recovered solid on the cold surface (5°C)

	1st sample OMW	2nd sample OMW	1st sample recovered solid	2nd sample recovered solid
COD (mg/L)	40,933	82,450	268	248
Phenolics (mg/L)	1980	2,992	6.25	6.2

from the carbohydrates. Literature search results were very promising suggesting the possibility of formation of solutions substantially enriched in phenolic content with a final concentration of hydroxytyrosol equal to 84.8 gL^{-1} [8]. As a final step, the cooling crystallization may be implemented for the selective recovery of purified crystalline PPs from OMW based on their respective freezing points [15].

4. Conclusions

The main objective of this current work was the development of viable, cost-effective treatment methods both for the efficient treatment of OMW and for the recovery of purified phenolic compounds. PPs may be exploited into different scientific domains, including pharmaceuticals, cosmetics etc., as these antioxidants are considered as high-added value products. Model experiments were done in which high recoveries (exceeding 60%) were obtained for TCA and FA upon imposing large temperature gradients between the bulk solution in the crystallizer (70°C) and a cooled cylindrical surface maintained at 5°C. From the experimental study carried out with mixtures of TCA and FA, it was found that the selective recovery of phenolic compounds is feasible through the cooling crystallization process, resulting to the crystallization of purified phenolic compounds on a cooled surface. The results of the present work have shown that cooling crystallization may be the final step for the development of a satisfactory model for the effective treatment of OMW stream.

The cooling crystallization of FA from model solutions in stirred solutions showed that high rotational velocities of the fluid phase, ω , had negative effects on the final PP recovery. Crystallization in the bulk, as a result of high fluid flow, may account for the lower recovery at higher values of the rotational velocity of the fluid in the crystallizer.

As a final comment, it should be emphasized that the isolation of phenolic compounds from OMW, aims at concentrating them to adequately high concentration levels. Combination of several physicochemical treatment methods is necessary in order to obtain a final bulk solution enriched in PP fractions.

Acknowledgments

The present work is part of the project 'Theoretical and experimental study of the controlled precipitation of inorganic salts in granular and consolidated porous media, SPM,' which is implemented within the 'ARISTEIA II' Action of the 'OPERATIONAL PROGRAMME EDUCATION AND LIFELONG LEARNING.' Assistance in the crystallization experiments by Grigorios Stelios is acknowledged.

References

- [1] H. Zbakh, A. El Abbassi, Potential use of olive mill wastewater in the preparation of functional beverages: A review, *J. Funct. Foods* 4 (2012) 53–65.
- [2] I. Fki, M. Bouaziz, Z. Sahnoun, S. Sayadi, Hypocholesterolemic effects of phenolic-rich extracts of *Chemlali* olive cultivar in rats fed a cholesterol-rich diet, *Bioorg. Med. Chem.* 13 (2005) 5362–5370.
- [3] E.C. Arvaniti, D.P. Zagklis, V.G. Papadakis, C.A. Paraskeva, High-added value materials production from OMW: A technical and economical optimization, *Int. J. Chem. Eng.* 2012 (2012) 7.
- [4] G. Rana, M. Rinaldi, M. Intron, Volatilisation of substances after spreading olive oil waste water on the soil in a Mediterranean environment, *Agric. Ecosyst. Environ.* 96 (2003) 49–58.
- [5] I.C. Iakovides, A.G. Pantziaros, D.P. Zagklis, C.A. Paraskeva, Effect of electrolytes/polyelectrolytes on the removal of solids and organics from olive mill wastewater, *J. Chem. Technol. Biotechnol.* (2014), doi: 10.1002/jctb.4563.
- [6] C.A. Paraskeva, V.G. Papadakis, E. Tsarouchi, D.G. Kanellopoulou, P.G. Koutsoukos, Membrane processing for olive mill wastewater fractionation, *Desalination* 213 (2007) 218–229.
- [7] C.A. Paraskeva, V.G. Papadakis, D.G. Kanellopoulou, P.G. Koutsoukos, K.C. Angelopoulos, Membrane filtration of olive mill wastewater and exploitation of its fractions, *Water Environ. Res.* 79 (2007) 421–429.
- [8] D.P. Zagklis, A.I. Vavouraki, M.E. Kornaros, C.A. Paraskeva, Purification of olive mill wastewater phenols through membrane filtration and resin adsorption/desorption, *J. Hazard. Mater.* 285 (2015) 69–76.
- [9] A. Cassano, C. Conidi, E. Drioli, Comparison of the performance of UF membranes in olive mill wastewaters treatment, *Water Res.* 45 (2011) 3197–3204.
- [10] A. Cassano, C. Conidi, Fractionation of olive mill wastewaters by membrane separation techniques, *J. Hazard. Mater.* 248–249 (2013) 185–193.

- [11] Marco Stoller, Angelo Chianese, Optimization of membrane batch processes by means of the critical flux theory, *Desalination* 191 (2006) 62–70.
- [12] D.P. Zagklis, C.A. Paraskeva, Membrane filtration of agro-industrial wastewaters and isolation of organic compounds with high added values, *Water Sci. Technol.* 69 (2014) 202–207.
- [13] A. Chianese, N. Santilli, Modelling of the solid layer growth from melt crystallization—The integral formulation approach, *Chem. Eng. Sci.* 53 (1998) 107–111.
- [14] K.-J. Kim, J. Ulrich, Impurity distribution in a solid–liquid interface during static layer crystallization, *J. Colloid Interface Sci.* 252 (2002) 161–168.
- [15] S.S. Kontos, P.G. Koutsoukos, C.A. Paraskeva, Removal and recovery of phenolic compounds from olive mill wastewater by cooling crystallization, *Chem. Eng. J.* 251 (2014) 319–328.
- [16] L.S. Clesceri, A.E. Greenberg, R.R. Trusell, American Public Health, American Water Works, Water Pollution Control, Standard methods for the examination of water and wastewater, seventeenth ed., American Public Health Association, Washington DC, USA, 1989.
- [17] W.C. Johnson, A.H.A. Abbott, W.C. Wake, M.E. Dalziel, B. Atkinson, Abstracts of papers published in other journals. *Organic, Analyst* 74 (1949) 467–473.
- [18] M. Parisi, A. Chianese, The crystal layer growth from a well-mixed melt, *Chem. Eng. Sci.* 56 (2001) 4245–4256.
- [19] R.B. Bird, W.E. Stewart, E.N. Lightfoot, *Transport Phenomena*, Second ed., John Wiley & Sons, 2002, pp. 94–95 (Chapter 3).
- [20] K.A. Connors, The karl fischer titration of water, *Drug Dev. Ind. Pharm.* 14 (1988) 1891–1903.